Towards a MSG-based operational method for actual evaporation for Savannah regions in West Africa

A.F. Moene (1), D. Schüttemeyer (2) and H.A.R. de Bruin (1)[1]

(1) Meteorology and Air Quality Group, Wageningen University, The Netherlands,
(2) Meteorological Institute, University Bonn (MIUB), Germany

1. Introduction

For applications in water management, the estimation of actual evapotranspiration (ET) as one term in the water balance is critical. For operational water management of large river basins, the use of remote sensing estimates of actual ET is attractive. During the last decade, a large number of satellite algorithms have been developed to estimate actual ET. Most algorithms critically depend on the radiometric surface temperature and are therewith limited to cloud-free situations. This makes it difficult to obtain ET on a daily or weekly basis under the conditions in West Africa.

Schüttemeyer *et. al* (2007) (further referred to as SSMB07) presented a simple but robust algorithm based on the Makkink evaporation equation (based on ideas in Choudhury and DeBruin, 1995). The input data for the algorithm are remotely sensed incoming solar radiation, vegetation fraction and near-surface air temperature. However, the developed algorithm was applied for two test sites only and a number of shortcomings were identified by SSMB07 regarding processes and variability that were not taken into account. The present paper provides an extension of SSMB07 and shows a basin-wide application as well as an enhancement of the original method is presented. The focus of the application of the algorithm is on semi-arid regions, where variations in vegetation cover are large.

Section 2 describes the developed method, i.e. the original method plus enhancements. The input data used for this algorithm are described in section 3 and validation results are shown in section 4.

2. Description of the algorithm

2.1. Model for actual evaporation

In the interest of clarity, some basic quantities need to be defined in the context of ET estimation. Potential evaporation (PE) is the amount of water evaporated per unit area, per unit time from an idealized extensive free water surface under existing atmospheric conditions (Shuttleworth 1993). Optimal ET (OE) corresponds to the ability of plants to transpire under ideal conditions (full vegetation cover, well watered) with a non-zero resistance to water vapor flux. Optimal ET is always lower then PE. Finally, one can estimate the actual ET (AE), which is dependent on actual vegetation cover and soil moisture status. The actual ET should equal optimal ET under ideal conditions.

One way to derive optimal ET which is not based on the radiometric temperature and is not necessarily a remote sensing technique is the crop factor method (Allen *et al.* 1998). For this approach, the optimal ET is determined in the following way:

$$E_{opt} = k_c E_{ref}$$
(1)

where k_c is a crop factor and E_{ref} is the reference crop evaporation. The crop factor is an empirical quantity which is dependent on the type of vegetation, as well as on the phenology of the vegetation. Allen *et al.* (1998) discusses the values of k_c for a large range of crops as well as corrections for incomplete cover, mixed crops and phenology. For the estimation of E_{ref} the Penman-Monteith equation (e.g. Allen *et al.* 1998, 2000) is utilized. It requires the input of net radiation, air temperature, humidity and wind speed. Most of these input variables are not readily available and difficult to derive from remote sensing data. The estimation of net radiation in particular can cause large errors, since it cannot be obtained directly from remotely sensed measurements and the surface conditions for the studied region change noticeable during the year.

An alternative and simpler way of deriving reference ET is the approach developed by Makkink, who found that the equation of Penman could be simplified. De Bruin (1987) showed that the Makkink

---

[1] Retired as of June 2007

formula can also be 'derived' from the empirical formula of Priestley and Taylor and modified it accordingly. With this modified Makkink formula, the reference ET can be defined as follows:

$$L_v E_{ref} = 0.65 \frac{s}{s+\gamma} R_s \qquad (2)$$

where L_v is the latent heat of vaporation in J kg^{-1}, R_s is the incoming solar radiation in W m^{-2}, s is the slope of water vapor pressure at constant temperature and γ is the psychrometric constant (both in Pa K^{-1}).

The total ET from a partly vegetated surface can be regarded as being the sum of transpiration by the plants (controlled by the stomata) and bare soil evaporation. If the incomplete cover has not been taken into account in the crop factor, the total actual evaporation can be estimated as:

$$E_{act} = VF \cdot \left(E_{opt} + E_{intercept} \right) + (1 - VF) \cdot E_{soil} \qquad (3)$$

Here *VF* is the actual green vegetation fraction. For dry vegetation, $E_{intercept}$ is zero, whereas for wet vegetation E_{opt} is zero (see section 2.2.2). The introduction of *VF* could be interpreted as a modification of the crop factor to take into account incomplete cover (see Allen *et al.* (1998) for more elaborate corrections for incomplete cover). Justification for applying this modified Makkink approach is that in the semi-arid regions, vegetation adjusts its cover directly to the available water: if there is less water to evaporate, this will be reflected in the vegetation cover. The present method only reacts to changes in the vegetation cover. In case the vegetation suffers water stress and closes its stomata, this will not be reflected in the estimated actual evaporation.

2.2. Submodels

The validation performed in SSMB07 comprises mainly the dry part of the season and evaporation of intercepted water from vegetation and bare soil evaporation should be small. A basinwide application for longer time scales a number of quantities need further specification, viz. the crop factor, evaporation from intercepted water and bare soil evaporation

2.2.1. Variation of the crop factor based with land cover type

In SSMB07 the crop factor was set to unity for the vegetation under consideration (savannah). In SSMB07 it is clearly detectable, that actual evaporation is underestimated for nearly the entire range of measured ET. To improve the quality of the SSMB07 algorithm it is therefore crucial to introduce a more general concept to take different types of vegetation into account (not only the vegetation cover). To introduce the crop factor we mainly followed the ideas of Allen *et al.* (1998, 2000). We have assigned crop factors to different classes of vegetation cover. The general guideline in assigning crop factors to vegetation classes is given in Table 1.

Vegetation Type	Crop factor
low vegetation	1
high vegetation	1.2
savannah (mixture of low and high, and based on own data):	1.15
open water	1.25

Table 1: Crop factors for various surface cover types

The value of k_c for open water is based on the relationship between the crop factors for Penmen (open water) and Makkink (reference grass) as obtained for the Netherlands (see De Bruin and Lablans (1998)). For deep open water, the will be a phase shift between the radiation input and the evaporation, and the direct link between E_{opt} and E_{ref} will become invalid.

2.2.2. Interception by vegetation

In general interception is defined as that part of the precipitation on the canopy that does not reach the ground, because it evaporates from the canopy. The amount of interception critically depends on different meteorological factors like precipitation intensity, precipitation duration and wind speed. In the the present model interception from vegetation is calculated using Hortons's model adopted for partial canopy cover (Horton, 1919) and elaborated by Gash *et al.* (1995):

$$I = VF \cdot \min \left(P, aP + b \right) \qquad (4)$$

where *P* is the daily precipitation in mm and *a* and *b* are parameters determined by vegetation cover and precipitation characteristics. The actual values of *a* and *b* are given in Table 2.

Vegetation Type	a	b
Tall Vegetation Broadleaf (tropical)	0.05	1
Short Vegetation (tropical)	0.02	0.7

Table 2: **Values for coefficients involved in calculation of interception by vegetation.**

The evaporation of intercepted water is assumed to take place in the following stages. Intercepted water is evaporated at the day of the rainfall (and not thereafter):

- If the amount of intercepted water is less than the open water evaporation ($VF \cdot k_c E_{ref}$ with k_c is taken as the open water crop factor) all of the intercepted water is evaporated and the remaining energy is used for transpiration with the appropriate crop factor.
- If the amount of intercepted water is larger than the open water the amount of evaporation equals the open water evaporation.

2.2.3. Bare soil evaporation

Bare soil evaporation is an important process especially during the wet part of the season, and for those regions where large areas are covered with savannah type vegetation and are not fully vegetated. Wallace and Holwill (1997) and Wallace *et al.* (1992) analyzed bare soil evaporation within HAPEX-Sahel and found that rapid drying of the soil led to values of maximal 0.5 mm d^{-1} after one week. Additionally Gash *et al.* (1997) found that bare soil evaporation decreased to less than 20% of total evaporation within two days after a rain event. This shows that the errors would be largest following the day immediately after the rain but would also lead to a small bias after a few days without rain. Therefore bare soil evaporation is modeled to occur in two stages (Ritchie 1972); the first stage being energy limited, the second stage being exfiltration limited. The first stage is only taken into account for the day following the actual rainfall. During that day the actual evaporation equals the reference evaporation determined by equation (2). The second stage is calculated using the formulation of Ritchie (1972):

$$E_{soil2} = s[t^{0.5} - (t-1)^{0.5}] \qquad (5)$$

where *s* is the desorptivity (mm day$^{-0.5}$) and *t* is time (days) elapsed since the day following the rainfall. In general the desorptivity is in the range of 3-5 mm day$^{-0.5}$. Based on the analyses within HAPEX-Sahel mentioned above and a simple sensitivity analysis combined with the limited amount of measurements we adopted a value of 3 mm day$^{-0.5}$.

In the algorithm, bare soil evaporation starts at the first day after rain and takes place at the bare soil fraction (1-*VF*) only.

3. Data

Satellite data are widely applied for the determination of atmospheric and surface properties. Depending on the satellite system, the spatial and temporal resolution can range from tens of meters to several kilometers and from half-hourly to half-daily images.

3.1. Incoming solar radiation

Many approaches exist to derive the incoming solar radiation at ground level using geostationary satellite data. Most methods relate the reflected sunlight measured by the METEOSAT VIS channel covering the range 0.45 μm - 1.0 μm to the incoming solar radiation at the surface of the earth. The method used in this study has been described in Perez *et al.* (2002), which derives it as an evolution of the model of Cano *et al.* (1986) (see also Mannstein *et al.* 1999). This method was developed for the determination of incoming solar radiation using data from the geostationary satellite GOES (Geostationary Operational Environmental Satellite). For this study, data from the VIS channel of METEOSAT-7 were adapted and included in the calculation scheme. Details on the method, as well as validation results, can be found in SSMB07.

A more recent, alternative source of incoming solar radiation data is the product the Land Surface Analysis Satellite Applications Facility (LSA SAF) which provides incoming solar radiation data on an operational basis, based on MSG-data.

3.2. Near-surface temperature

For the determination of the reference evaporation, the air temperature at screen level is needed. In the present study, a reference-temperature has been used which is a by-product of the cloud-detection scheme used for the determination of global radiation. In SSMB07 it was shown that this reference temperature correlates well (with a bias) with observed air temperatures.

The near surface temperature could also be obtained from atmospheric model data. Although the model input might be imperfect, the impact on the calculated evpotranspiration would be minor, given the fact that T is only used to calculate s.

3.3. Green vegetation fraction

In the present method, the vegetation fraction is derived from the enhanced vegetation index (EVI), which is an operational product derived from MODIS data. EVI was developed to take into account the influence of both the atmosphere and the soil on the vegetation index (Liu and Huete 1995). If the maximum value of EVI (EVI_{max}) is assumed to be the EVI of vegetation, and the minimum value (EVI_{min}) is assumed to be the background value, the vegetation fraction can be determined as:

$$VF = \frac{EVI - EVI_{min}}{EVI_{max} - EVI_{min}}$$

(6)

This linear dependence is based on the quadratic dependence of VF on a scaled NDVI (e.g. Carlson and Ripley 1997), in combination with an approximate quadratic relationship of EVI and NDVI as is apparent from the images we have used. More details on the derivation of VF from MODIS data, as well as on collocation of METEOSAT and MODIS data can be found in SSMB07.

An alternative source of VF data could be the use of the vegetation fraction product, currently under development by LSA-SAF.

3.4. Crop factor

As a first basis for crop factor estimation the USGS database was utilized. The original data is based on 1-km AVHRR data with 1-km nominal spatial resolution and here we used the 30-second resolution database that comes with the MM5-model. In order to obtain a vegetation cover map at the required resolution, the modal cover type within an output pixel was taken. Based on the different land use classification within the USGS database the crop factors were introduced. In a second step the measurements obtained during 2002 (see SSMB07) were utilized to provide a solid basis for the crop factor for savannah type vegetation.

USGS land use classes for the use of the crop factors in AE estimation		crop factor
1-9	Urban and Built-Up Land, Dryland Cropland and Pasture, Irrigated Cropland and Pasture, Mixed Dryland/Irrigated Cropland and Pasture, Cropland/Grassland Mosaic, Cropland/Woodland Mosaic, Grassland, Shrubland, Mixed Shrubland/Grassland	1.00
10	Savanna	1.15
11-15	Deciduous Broadleaf Forest, Deciduous Needleleaf Forest, Evergreen Broadleaf Forest, Evergreen Needleleaf Forest, Mixed Forest	1.20
16	Water Bodies	1.25
17-24	Herbaceous Wetland, Wooded Wetland, Barren or Sparsely Vegetated, Herbaceous Tundra, Wooded Tundra, Mixed Tundra, Bare Ground Tundra, Snow or Ice	1.00

Table 3: **Assignment of crop factors to land cover classes**

3.5. Satellite based precipitation estimates

Near real-time rain fall information obtained from remote sensing data (RFE 2.0, a product of NOAA) has been included to serve as input for the parameterization of evaporation from interception and bare soil. The input data used for the operational rainfall estimates for RFE 2.0 are obtained from 4 different sources:

1) Daily GTS rain gauge data for up to 1000 stations in Africa
2) AM SU microwave satellite precipitation estimates up to 4 times per d ay
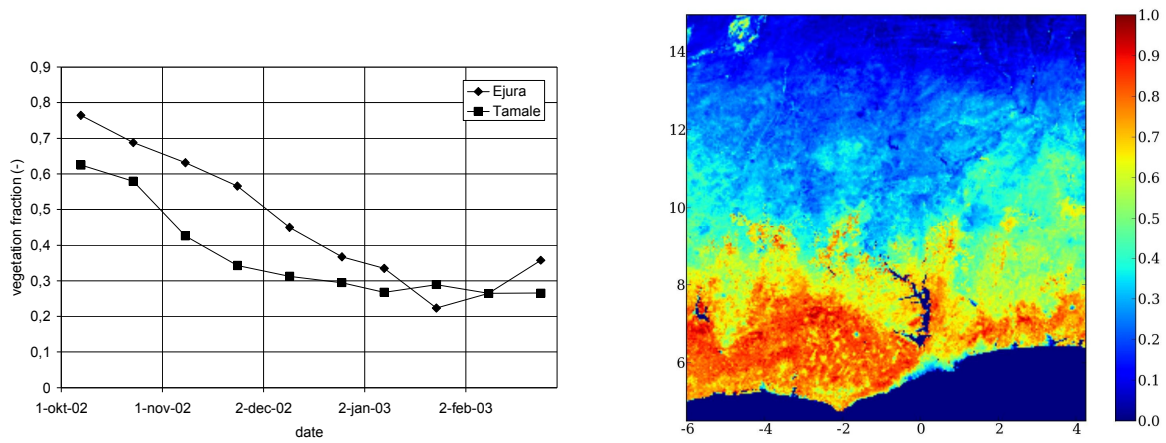3) SSM /I satellite rainfall estimates up to 4 times per day

Figure 1: Left: temporal evolution of green vegetation fraction for the two test sites. Results are averaged over 4 adjacent pixels, surrounding the sites, for those pixels where no clouds contaminated the 16 days composite. Right: vegetation fraction for November 15, 2002.

    4)   GPI cloud-top IR temperature precipitation estimates on a half-hour basis.

The three satellite estimates are first combined linearly using predetermined weighting coefficients, then are merged with station data to determine the final African rainfall. Daily binary and graphical output files are produced at approximately 3pm EST with a resolution of 0.1° and spatial extent from 40°S 40°N and 20°W-55°E.

4.   Results

The method presented in section 2 has been applied using hourly estimates of incoming solar radiatjon and near-surface temperature, 16-day composites of *VF* and daily rainfall estimates from RFE. The validation in section 4.1 has been performed on hourly fluxes, whereas the presentation of spatial fields in section 4.2 is based on daily sums and monthly sums.

4.1. Validation

Full validation of the various components of the present algorithm is beyond the scope of this paper. Part of this validation (regarding incoming solar radiation and near surface temperature, as well ET from the original method) can be found in SSMB07.

Validation of the actual ET is performed using data obtained in the framework of the GLOWA-Volta project. The measurements involved a large aperture scintillometer (LAS) to observe sensible heat flux, measurement of net radiation and and soil heat flux. The latent heat flux (i.e. ET) was determined as a residual from the energy balance. Data from two sites are used: Ejura (7°20′ N; 1°16′ W), Tamale
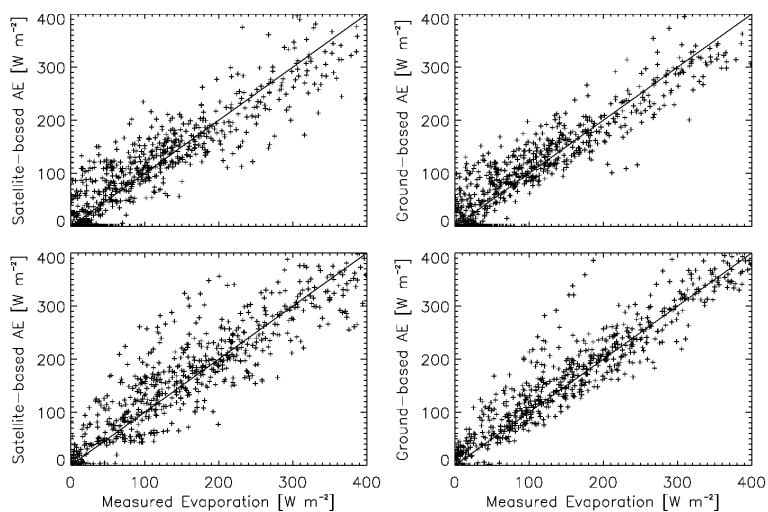

Figure 2: Left: Satellite-based AE vs. measured scatterplot for the analyzed periods at the two sites (Tamale (top) and Ejura (bottom). Right: Direct comparison of the remote sensing algorithm with ground-based solar radiation and temperature vs. measured AE at the two sites.
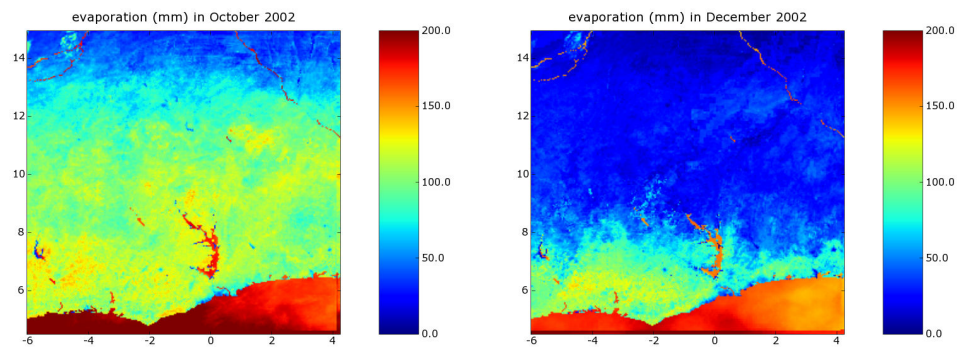
Figure 3: Monthly sum of evapotranspiration for October (left) and December (right) 2002.

(9°29′ N, 0°55′ W). For more details see Schüttemeyer *et al.* (2006) and SSMB07.

The validation was performed for the period from August 26, 2002 to December 31, 2002. The period covered the transition from the wet to the dry season in the studied region. The study period itself contained only few (Ejura) to no (Tamale) rain events, and thus the skill of the estimations of bare soil and interception evaporation could not be assessed.

In order to evaluate if the vegetation fraction is - in this case - an important factor in the estimation of actual evaporation, we first evaluated the spatial and temporal variation of the vegetation fraction as estimated from the MODIS data. Figure 1 shows the temporal development of *VF* for the sites, as well as the spatial distribution of VF for the entire Volta Basin. It is apparent that the change in *VF* through the season was very large for all sites (from around 0.7 to 0.25). Furthermore, the most-southern site (Ejura) had a significantly higher *VF* for most of the season, until mid January. Both the temporal and spatial variation of *VF* will impact on the variation of AE.

Figure 2 shows a comparison of hourly evaporation rates (latent heat flux) as measured in the field and as derived from the remote sensing algorithm. The scatter is of the same order as when two independent micrometeorological methods for flux measurements are compared. In the right part of Figure 2 the remote sensing algorithm has been fed with locally observed incoming solar radiation and temperature data (henceforth ground-based AE). The scatter that remains as compared to the left figure is an indication of the mismatch between locally observed global radiation and temperature and the values derived with remote sensing (partly due to scale differences between METEOSAT data and point observations.
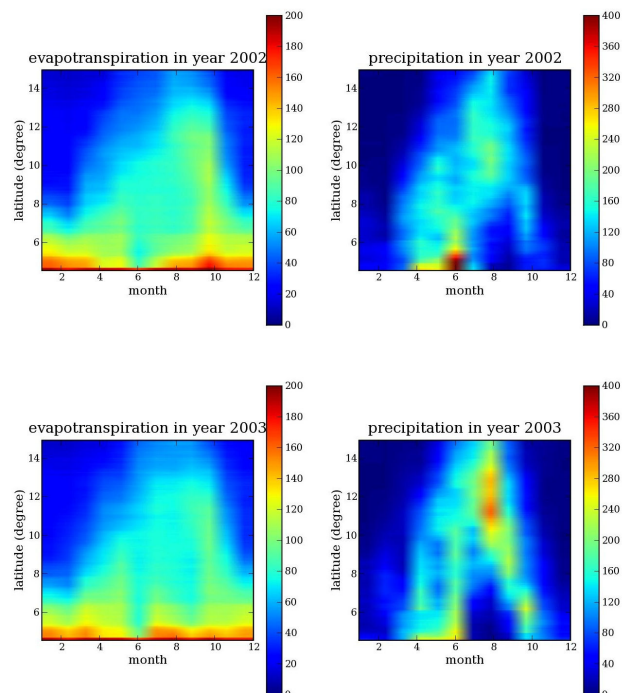

Figure 4: Zonal mean evapotranspiration (left) and precipitation (right) for the years 2002 (top) and 2003 (bottom). The values signify monthly sums in mm.

4.2. Results for the Volta Basin

The method presented in this paper has been applied for a region of roughly 1250 times 1250 kilometers, encompassing the basin of the Volta river, for the years 2002 and 2003.

Figure 3 shows the ET sum for two exemplary months in 2002: October, which is the start of the dry season in the North, and December when vegetation has decreased significantly (see figure 1). October and December 2002 are also the first and last month of the observations used in figure 2. Cleary visible in both maps is the high evaporation from the ocean and Lake Volta, as well as flooding areas e.g. Macina in Mali and larger rivers. Furthermore, the north-south gradient in ET is clearly visible, especially in December.

Figure 4 shows the zonally and monthly averaged ET and precipitation for two years. The high evaporation rates of the sea are visible in the south (up to approx. 6°N). The south to north migration of higher evaporation rates in March to May (and the retreat from October to December) is clearly visible. Furthermore, the evaporation rises following the first rain events in the season: the higher evaporation rates seem to precede the high rain rates: the first rains are sufficient to start vegetation growth and subsequent evaporation. In the dry season the evaporation is limited by availability of water, whereas in the rainy (cloudy) season the evaporation is energy limited. This is also visible in the high evaporation rates in October for a large range of latitudes: sufficient water is available, and the cloudiness has decreased. The decline of evaporation in the dry season lags the end of the rains by approximately one month.

5. Discussion and outlook

The tested method is intended as a first-order approach to estimate ET for an entire season on a daily basis, without needing to exclude partly cloudy situations. In contrast, methods that use a remotely sensed surface temperature to estimate surface fluxes have problems under partly cloudy conditions, because the scattered clouds can easily contaminate the estimated surface temperature if the cloud-detection scheme misses the clouds.

The method presented here includes all the important factors that influence ET from land surfaces with varying mixtures of vegetation and bare soil:

- the type of vegetation
- the part of the surface covered with vegetation
- bare soil evaporation
- evaporation from intercepted water
- the radiative forcing

Those influences also reflect decreasing time scales from multi-year cycles to the diurnal cycle.

It was shown that certain limits exist when such a first-order approach is applied. The first limit is related to the use of Makkink's equation which makes use of incoming solar radiation rather than net radiation for estimating optimal ET. Furthermore eventual effects of wind speed and humidity in the atmosphere were neglected.

The results suggest that the simple satellite-based method is also suitable to verify meteorological models in regions under consideration where ground-truth weather data are scarce. A small network of scintillometers might be added to validate the satellite-based algorithm at a limited number of sites.

The full potential of the spatially varying crop factor can only be exploited if near realtime databases exist. Therefore the USGS database should be replaced by the land use classes developed within the GLOWA-Volta project, or other sources of land used (e.g. MODIS land cover). Furthermore Allen *et al.* (1998) provides general lengths for the four distinct growth stages and the total growing period for various types of climates and locations. This might also lead to improved results for cultivated surfaces. In some situations, the time of emergence of vegetation and the time of effective full cover can be predicted using cumulative degree-based regression equations or by more sophisticated plant growth models (Allen *et al.*, 1998).

Finally, the current algorithm might be blended with a surface-temperature based scheme, where the latter provides information on the crop factor from cloudless scenes, and this 'observed' crop factor is used during cloudy conditions.

Acknowledgements

References

Allen, R.G., L.S. Pereira, D. Raes, and M. Smith, 1998: Crop ET: Guidelines for Computing Crop Water Requirements. FAO Irrig. and Drain. Paper, 56, Rome.

Allen, R.G., Walter, I.A., Elliott, R., Mecham, B., Jensen, M.E., Itenfisu, D., Howell, T.A., Snyder, R., Brown, P., Eching, S., Spofford, T., Hattendorf, M., Cuenca, R.H., Wright, J.L., and Martin, D. 2000. *Issues, requirements and challenges in selecting and specifying a standardized ET equation*. ASCE..

Cano, D., J.M. Monget , M. Albuisson, H. Guillard, N. Regas, and L. Wald, 1986: A method for the determination of the global solar radiation from meteorological satellite data. Sol. Energy, **37**, 31-39.

Carlson, T.N. and D.A. Ripley (1997). On the relation between NDVI, fractional vegetation cover, and leaf area index. *Remote Sens. Environ.* **62**, 241-252.

Choudhury, B.J., and H.A.R. De Bruin, 1995: First order approach for estimating unstressed transpiration from meteorological satellite data. *Adv. Space Res.*, **16**, pp. 167.

De Bruin, H.A.R., 1987: From Penman to Makkink, in J.C. Hooghart (Ed.), Evaporation and Weather, (*technical Meeting of the Committee for Hydrological Research, February, 1981*), Comm. Hydrol. Res. TNO, Den Haag, Proc. And Inform., **39**, 5-30.

De Bruin, H.A.R. and W.N. Lablans, 1998: Reference crop evapotranspiration determined with a modified Makkink equation. *Hydrol. Process.* **12**, p. 1053-1062.

Gash. I.H.C., Lloyd, C.R, Lachaud, G., 1995. Estimating sparse forest rainfall interception with an analytical model*, J. Hydrol.*, **170**, 79-86.

Gash, J.H.C., Kabat, P., Monteny, B.A., Amadou, M., Bessemoulin, P., Billing, H., Blyth, E.M., De Bruin, H.A.R., Elbers, J.A., Friborg, T., Harrison, G., Holwill, C.J., Lloyd, C.R., Lhomme, J.-P., Moncrieff, J.B., Puech, D., Soegaard, H., Taupin, J.D., Tuzet, A. and Verhoef, A., 1997. The variability of evaporation during the HAPEXSahel intensive observation period. *J. Hydrol.*, **188/189**, 385-399.

Horton, R.E., 1919. Rainfall interception, *Mon. Weather Rev.* **47**, 603-623.

Liu, H.Q. and A.R. Huete, 1995: A feedback based modification of the NDVI to minimize canopy background and atmospheric noise. IEEE. *Trans. Geosci. Remote Sensing,* **33**, 457-465.

Mannstein, H., C. Schillings, H. Broesamle and F. Trieb 1999: *Using a METEOSAT Cloud Index to Model the Performance of Solar Thermal Power Stations*. Presentation at EUMETSAT Conference, Copenhagen.

Perez R., P. Ineichen, K. Moore, M. Kmiecik, C. Chain, R. George and F. Vignola, 2002: A new operational satellite-to-irradiance model - description and validation. *Sol. Energy*, **73** (5), 307-317.

Ritchie, J.T. 1972. A model for predicting evaporation from a row crop with incomplete cover. *Water Resources Research* **8**(5), 1204-1214.

Schüttemeyer, D., A.F. Moene, A.A.M. Holtslag, H.A.R. de Bruin, and N. van de Giesen, 2005: Surface fluxes and characteristics of drying semi-arid terrain in West Africa. *Bound.-Layer Meteor.* **118** , p. 583 - 612.

Schüttemeyer, D., Ch. Schillings, A.F. Moene and H.A.R. de Bruin, 2005: Satellite-Based actual evapotranspiration over drying semiarid terrain in West-Africa. *Journal of Applied Meteorology and Climatology* **46**, p. 97 - 111.

Shuttleworth, W.J., 1993: *Evaporation. Handbook of Hydrology*, D.R. Maidment, Ed., McGraw-Hill, 4.1-4.53.

Wallace, J.S. and Holwill, C.J., 1997. Soil evaporation from tiger bush in South-West Niger. *J. Hydrol.*, **188/189**, 426–442.

Wallace, J.S., *et al.*., 1994. HAPEX-Sahel Southern Super-Site Report: An Overview of the Site and the Experimental Programme During the Intensive Observation Period in 1992. Institute of Hydrology, Wallingford, UK, 55 pp.